Applied Thermal Engineering 113 (2017) 481–489

Contents lists available at ScienceDirect

Applied Thermal Engineering

journal homepage: www.elsevier.com/locate/apthermeng

Research Paper

In-situ two-step Raman thermometry for thermal characterization of monolayer graphene interface material

Wenqiang Zhao [a,b,1], Wen Chen [a,1], Yanan Yue [a,c,*], Shijing Wu [a,d,*]

[a] School of Power and Mechanical Engineering, Wuhan University, Wuhan, Hubei 430072, China
[b] Henan Pinggao Electric CO., Ltd, State Grid, Pingdingshan, Hehan 467000, China
[c] State Laboratory of Hydraulic Machinery Transients, Ministry of Education, Wuhan, Hubei 430072, China
[d] Key Laboratory of Water Jet Theory and New Technology of Hubei Province, Wuhan University, Wuhan, Hubei 430072, China

HIGHLIGHTS

- In-situ two-step Raman method is developed for interfacial thermal characterization.
- Both in-plane thermal conductivity and interface thermal conductance can be characterized.
- An unconstrained graphene/SiO_2 interface material is successfully measured.
- Small interface thermal conductance and in-plane thermal conductivity are obtained.

GRAPHICAL ABSTRACT

An in-situ two-step Raman thermometry is developed to measure both interfacial thermal conductance between graphene and substrate, and in-plane thermal conductivity of graphene.

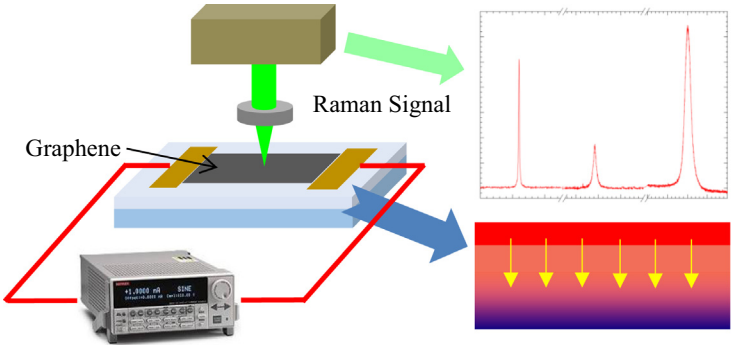

ARTICLE INFO

Article history:
Received 16 August 2016
Revised 5 November 2016
Accepted 8 November 2016
Available online 9 November 2016

Keywords:
Raman thermometry
Thermal conductivity
Interfacial thermal conductance
Graphene

ABSTRACT

To date, accurate thermal property measurement of atomic-layer interface materials still remains as a challenge due to the extreme dimension of sample's size and limitation of instruments. Raman thermometry emerges as the sole technique for direct measurement of unconstrained graphene interfacial thermal transport. In this work, an in-situ two-step Raman thermometry is developed to measure both interfacial thermal conductance between graphene and substrate, and in-plane thermal conductivity of supported graphene. This two-step Raman approach incorporates the first step: joule-heating experiment for interfacial thermal conductance characterization and the second step: laser-heating experiment for thermal conductivity measurement. Thermal conductance between monolayer graphene and SiO_2 is characterized as 340^{+327}_{-80} W/m^2 K which is much smaller than reported values of sandwiched graphene interface structures, but agrees well with other unconstrained graphene interface structures. The in-plane thermal conductivity of supported graphene is obtained as 179^{+111}_{-86} W/m K. This value is consistent with previously reported data for thermal transport of supported graphene structures, which can be explained by phonons leakage and significant scattering at the interface. The successful measurement of graphene/SiO_2 interfacial thermal properties proves that this technique can be well applied to graphene-like atomic-layer materials with Raman-active optical mode.

* Corresponding authors at: School of Power and Mechanical Engineering, Wuhan University, Wuhan, Hubei 430072, China.
E-mail addresses: yyue@whu.edu.cn (Y. Yue), wsj@whu.edu.cn (S. Wu).
[1] These authors contribute equally.

http://dx.doi.org/10.1016/j.applthermaleng.2016.11.063
1359-4311/

Nomenclature

R_{in}	thermal resistance (m^2 K/W)
L	length (m)
k	thermal conductivity (W/m K)
A_{cr}	cross-sectional area (m^2)
R_{out}	total interfacial thermal resistance (m^2 K/W)
R_{g/SiO_2}	area interfacial thermal resistance (m^2 K/W)
A	contact area (m^2)
$\Delta T_{g/SiO_2}$, $\Delta T_{Si/SiO_2}$	temperature drop (K)
Q	joule-heating power (W)
q	heat flux (W/m^2)
h	interfacial thermal conductance (W/m^2 K)
r_1,r_2	radius (m)
I_0, K_0, I_1, K_1	Bessel functions
t_{Si}, t_g	slope (cm^{-1}/K)
R_{Si/SiO_2}	thermal resistance (m^2 K/W)
q_{Si}, q_g	slope (cm^{-1}/W)
G_{g/SiO_2}	interfacial thermal conductance (W/m^2 K)

Greek symbols

δ	thickness (m)
θ	temperature rise (K)

Subscripts

in	in-plane
out	out-plane
g/SiO_2	interface between graphene and SiO_2
Si/SiO_2	interface between Si and SiO_2

1. Introduction

As nanoelectronic devices are continuously miniaturized and the demand for power density dissipation is increased, there are serious problems in thermal management [1]. Graphene emerges as a perfect candidate in thermal management of nanoelectronic devices for its superb thermal property [2]. Thermal transport in graphene has attracted much attention in the last decade [3–5]. Kong et al. [6] reported the thermal conductivity of monolayer graphene was 2200 W/m K at 300 K by first principle calculations. Thermal conductivity of suspended single-layer graphene is characterized as an extremely high value of 5300 W/m K at room temperature [7]. Molecular dynamics simulations obtained ultrahigh thermal conductivity of graphene sheets in the order of 1000 W/m K at room temperature [8]. Benefiting from its ultrahigh thermal conductivity, graphene and graphene-based materials have shown great advantages of applications in nanoelectronic devices [9–12]. In almost all practices, graphene is either supported by substrates or encased in dielectrics, while suspended graphene and free-standing graphene are not common in practical devices. Different from superb and unconstrained heat dissipation of suspended graphene in the in-plane direction, heat dissipation of supported and encased graphene in the in-plane direction is impacted by the interfacial thermal transport between graphene and substrates; in other words, thermal conductivity of supported graphene in the in-plane direction is affected by phonon interaction at the interface [13].

Until now, several works about thermal characterization of graphene in the in-plane direction have been reported [13–15]. When graphene is supported by substrates or encased in dielectrics, coupling and scattering of phonons with substrates could greatly suppress thermal conductivity of graphene in the in-plane direction. Seol et al. [13] reported that thermal conductivity of graphene supported by silicon dioxide was about 600 W/m K near room temperature. Jang et al. [14] utilized the model of a single-layer graphene sandwiched between two silicon dioxide layers and obtained the thermal conductivity of graphene below 160 W/m K using a heat spreader method. Chen et al. [15] studied the effects of sample size, the thickness of graphene layers and coupling strength with substrate on thermal conductivity of graphene supported by an amorphous silicon dioxide substrate using molecular dynamics (MD) simulations and determined that the thermal conductivity of supported single-layer graphene was 609 ± 19 W/m K. Thus, the in-plane thermal transport of supported graphene is not as efficient as perfect suspended graphene for heat dissipation in nanoelectronic devices. Meanwhile, there is remarkable thermal resistance existing at graphene/substrate interface. Several studies about heat transport across the interfaces between graphene and substrates have been reported [16–19]. Atomistic modelling approaches including first principles [16] and molecular dynamics simulations [17] were conducted to study thermal transport between graphene and SiC, and the interfacial thermal conductance was predicted at the order of magnitude of 10^7–10^9 W/m^2 K. Chen et al. [18] revealed the interfacial thermal conductance between engaged graphene and silicon dioxide ranged from 8.3×10^7 to 1.8×10^8 W/m^2 K using a differential 3ω method. Koh et al. [19] measured the interfacial thermal conductance at graphene/SiO_2 interface from Au/Ti/graphene/SiO_2 structure by pump probe method and found the interfacial thermal conductance approximated 2.5×10^7 W/m^2 K. Tang et al. [20] used Raman thermometry to investigate the thermal transport across unconstrained graphene/Si and graphene/SiO_2 interfaces. The values of interfacial thermal conductance were obtained as 183 and 266 W/m^2 K respectively, much lower than the interfacial thermal conductance of constrained graphene/substrate interfaces and theoretically predicted values.

Most works about thermal transport in graphene/substrate system solely focus on either in-plane thermal conductivity or cross-plane interfacial thermal conductance as mentioned above. However, it should be regarded as an integrated process since heat dissipation at interface between graphene and substrate and in-plane thermal transport of graphene are coupled effect as a heat spot is generated. Thus, two thermal transport channels should be explored simultaneously to comprehensively understand thermal transport in graphene/substrate system. There are a few of works about thermal transport in in-plane direction of graphene and across the interfaces between graphene and substrates, but only few works have been conducted on investigation of both thermal conductivity and interfacial thermal conductance between graphene and substrate. Cai et al. [21] and Judek et al. [22] succeed in this kind of characterization based on Raman spectroscopy. In this work, we proposed a two-step approach based on Raman thermometry for localized measurement of both thermal conductivity of graphene and interfacial thermal conductance between graphene and substrate.

2. Experimental principle and details

2.1. First step (joule-heating) experiment principle

As shown in Fig. 1(a), both ends of graphene flake are connected to electrodes by silver paste for joule-heating. Constant current is

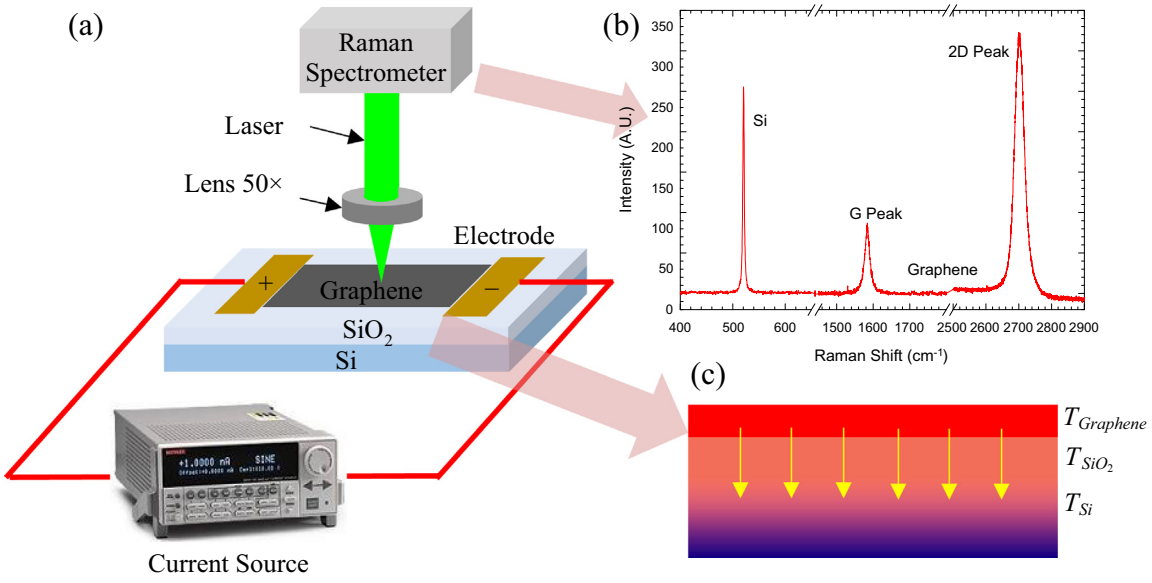

Fig. 1. (a) Schematic of thermal characterization of graphene/SiO_2 interface by using two-step Raman method. The graphene layer is connected to electrodes for steady state joule heating. Probing laser is focused on graphene layer to characterize Raman signal of interface materials to get temperature difference. (b) Typical Raman spectrums of graphene and silicon obtained in the experiment, and the Raman signal of SiO_2 is not obvious in the spectrum. (c) The schematic of heat dissipation under joule heating. There is uniform heating effect generated in graphene which dissipates across the interface.

supplied to generate uniform heating effect inside graphene. There are several channels for heat dissipation: heat dissipation to air through heat convection, thermal radiation to surrounding environment, heat conduction to the electrodes, and thermal transport across graphene/SiO_2 interface. The natural convection coefficient is less than 10 W/m^2 K [23] which is far below the equivalent interfacial thermal conductance (around 300 W/m^2 K calculated from the values in Table 1). Meanwhile, the radiation heat loss is closely related to the temperature rise of the sample which is less than 200 °C in our experiment. The radiation heat loss calculated from this temperature rise is also incomparable to heat transport across the interface. According to Table 2, assuming that thermal conductivity of graphene can reach as large as 1×10^4 W/m K, the minimum value of thermal resistance of in-plane direction is estimated as $R_{in} = L/kA_{cr} \approx 3 \times 10^5$ K/W, where L is the length of graphene, k is thermal conductivity, A_{cr} is the cross-sectional area, respectively. Meanwhile, the total interfacial thermal resistance between graphene and SiO_2 is estimated at the order of $R_{out} = R_{g/SiO_2}/A = 1 \times 10^2$ K/W, where R_{g/SiO_2} is the area interfacial thermal resistance around 10^{-2} m^2 K/W according to Table 1, and A is contact area. The in-plane thermal resistance is far more than that in out-of-plane direction, which indicates that joule-heating power dissipates mainly through the interface. The thermal resistance between graphene and substrate is calculated as $R_{g/SiO_2} = A\Delta T_{g/SiO_2}/Q$ where Q is the joule-heating power, $\Delta T_{g/SiO_2}$ is the temperature drop between graphene layer and SiO_2 layer, respectively.

Raman spectroscopy is a traditional material characterization method, but has been widely applied in thermal characterization in recent years, especially on carbon based low dimensional materials [24–27]. The principle is very simple: Raman signal is temperature dependent, which shows in the spectrum as the Raman peaks shift to the low wavenumber direction as temperature is increased for most crystalline materials. Thus it can be used as a tool for temperature probing. For example, it has been applied in the neat-field optics focusing for measuring localized temperature with dimensional down to sub 10 nm [28]. In this work, Raman thermometry is used by focusing the probing laser on the graphene flake due to its ultrathin thickness and sound signals. It needs to be consistent since little variation of focusing level might change the heating from the laser and captured Raman signal, which induces measurement uncertainty. As Raman laser is focused on the graphene layer, it can penetrate very thin SiO_2 layer into silicon substrate [29]. Different Raman signals for these layers can be obtained as shown in Fig. 1(b). Typical Raman spectrum of the sample consists of three peaks, two of which are G peak at ~1580 cm^{-1} and 2D peak at ~2700 cm^{-1} for graphene and another one is at ~520 cm^{-1} for silicon. The intensity ratio of G peak to 2D peak is around 0.11, which indicates that the graphene flake has a mono-layer structure [30].

Table 1
Selected interfacial thermal conductance results between graphene and substrates.

	Materials	Methods	G (W/m^2 K)
Chen et al. [18]	Au/SiO_2/graphene/SiO_2/Si	Differential 3ω method	$(0.8–1.8) \times 10^8$
Koh et al. [19]	Au/Ti/graphene/SiO_2	Pump probe	2.5×10^7
Mak et al. [46]	Graphene/SiO_2	Pump probe	5×10^7
Cai et al. [21]	Graphene/Au/SiN_x/Si	Raman spectroscopy	2.8×10^7
Judek et al. [22]	Graphene/SiO_2/Si	Opto-thermal method	1.7×10^6
Hopkins et al. [47]	Al/graphene/SiO_2	Pump probe	3×10^7
Tang et al. [20]	Graphene/SiO_2	Raman spectroscopy	266
This work	Graphene/SiO_2/Si	Raman spectroscopy	340

Table 2
Selected thermal conductivity results of supported graphene and suspended graphene.

	Materials	Methods	k (W/m K)
Balandin et al. [7]	Suspended graphene	Raman spectroscopy	5300
Wang et al. [48]	Suspended graphene	T-type sensor method	2100
Lee et al. [49]	Suspended graphene	Raman spectroscopy	1800
Xu et al. [50]	Suspended graphene	Thermal bridge	1689–1813
Faugeras et al. [51]	Suspended graphene	Raman spectroscopy	632
Cai [21]	Graphene/Au/SiN_x/Si	Raman spectroscopy	370
	Suspended graphene	Raman spectroscopy	2500
Wang et al. [52]	Pt/graphene/SiO_2/Si	Thermal bridge	1250
Seol [13]	Graphene/SiO_2	Raman spectroscopy	600
Judek [22]	Graphene/SiO_2/Si	Opto-thermal method	335
Jang [14]	SiO_2/graphene/SiO_2/Si	Heat spreader method	160
This work	Graphene/SiO_2/Si	Raman spectroscopy	179

2.2. Second step (laser-heating) experimental principle

Unlike joule-heating experiment, in localized laser-heating experiment, thermal response of graphene is determined by both the in-plane thermal conductivity and interfacial thermal conductance. Similar to the joule-heating experiment, the probing laser is focused on graphene. However, laser energy is more intensive and is the sole heat source for graphene. The thermal transport process in graphene heated by laser is described as [23]

$$q = 2\pi k r_1 \delta \theta m \frac{K_1(mr_1)I_1(mr_2) - K_1(mr_2)I_1(mr_1)}{K_0(mr_1)I_1(mr_2) + K_1(mr_2)I_0(mr_1)} \quad (1)$$

where q is the heat flux across boundary of the heated section of graphene, k is the thermal conductivity of graphene, δ is the in-plane thickness of the unheated part of graphene, θ is the temperature rise at boundary of the heated section of graphene, $m = \sqrt{2h/k\delta}$, h is the interfacial thermal conductance between graphene and SiO_2, r_1 is the radius of heated section of graphene, r_2 is the radius of unheated part of graphene, I_0, K_0, I_1, K_1 are the first and second kinds of zero-order and first-order Bessel functions [23]. The thermal conductivity of graphene can be calculated according to the laser power and temperature rise of graphene with other geometrical parameters.

2.3. Sample preparation

The graphene samples used in the experiment are synthesized by using chemical vapor deposition (CVD) method. Fig. 2(a) depicts the sample preparation process. Firstly, a 25-μm thick Cu foil (provided by Alfa Aesar, ω = 99.8%) is immersed in diluted hydrochloric acid for ten minutes to eliminate the oxides on its surface. Cu foil is placed in an evacuated tube furnace which is flowed through 20 sccm H_2 (g) under standard condition to maintain the pressure of 300 Pa. The temperature in the furnace is gradually elevated to 1050 °C in 30 min and sustained 1050 °C for another 30 min to ensure that the copper foil is annealed enough. CH_4 (g) with flow rate of 54 sccm flows through the furnace after annealing, and the flow rate of H_2 (g) is adjusted to 3 sccm. The pressure in the furnace is sustained 300 Pa for 3.5 min and 600 Pa for another 6.5 min. Graphene on Cu foil is prepared after the Cu foil cools down to room temperature promptly at atmosphere of H_2 (g). The next step is to remove the graphene flake from Cu foil by etching [31,32]. The poly-methyl methacrylate (PMMA) membrane is coated on the surface of graphene/Cu to form PMMA/graphene/Cu structure. Then it is baked at 120 °C in a heater for 30 min to improve adhesion between PMMA membrane and the graphene flake. After immersion in the $FeCl_3$/HCl solution for 8 h, the Cu foil is corroded thoroughly. It is washed for 10-min twice by diluted HCl solution and then for 10-min four times by deionized water. The washed PMMA/graphene film is transferred to the surface of Si/SiO_2 wafer to form the PMMA/graphene/SiO_2/Si structure. After natural drying, the PMMA/graphene/SiO_2/Si structure is immersed into acetone solution to remove the PMMA membrane. Finally, the graphene/SiO_2/Si sample is obtained and the Raman spectrum shows that there is monolayer graphene with low defect level. The sound Raman signal (G and 2D peaks) guarantees that Raman thermometry is a good option for thermal characterization.

2.4. Experimental details

Thermal experiment is performed on a LabRam HR confocal Raman spectrometer produced by HORIBA Jobin Yvon Inc. with resolution of 0.65 cm^{-1}. The dimension of graphene is 10 mm × 10 mm. The laser power is fixed at 0.14 mW for interfacial thermal conductance measurements and adjusted to different values for thermal conductivity measurements. The Raman laser is focused on materials through a 50× objective lens. The integration times for graphene and silicon are 30 s and 5 s respectively in consideration of the intensities of Raman signals of graphene and silicon. Each spectrum is averaged from three times measurements. In the joule-heating experiment, the heating power ranges from 0 mW to 840 mW by adjusting the current. Different Raman spectrums of graphene and Si are collected at different joule-heating currents, and each Raman spectrum is averaged from three times measurements. In the laser-heating experiment, the power ranged from 0.12 mW to 0.5 mW, and each Raman spectrum is averaged from three times measurements. During the experimental process, the sample is kept steady on the stage to ensure that probing position is consistent through joule-heating and laser-heating experiment.

3. Results and discussion

3.1. Calibration result of temperature coefficient

Raman thermometry has been widely applied in thermal characterization experiments by assuming its linear relationship between Raman shift and temperature within a small temperature range [7,33,34]. Balandin et al. [7] conducted the first thermal conductivity measurement of single-layer graphene and revealed its ultrahigh thermal conductivity. Yoon et al. [33] estimated the thermal expansion coefficient of single-layer graphene with Raman spectroscopy. Yue et al. [34] succeeded in measuring the interfacial thermal resistance between epitaxial graphene and SiC substrate via Raman thermometry. Considering that the qualities (defects, doping, strain, etc.) of samples and different lasers, calibration

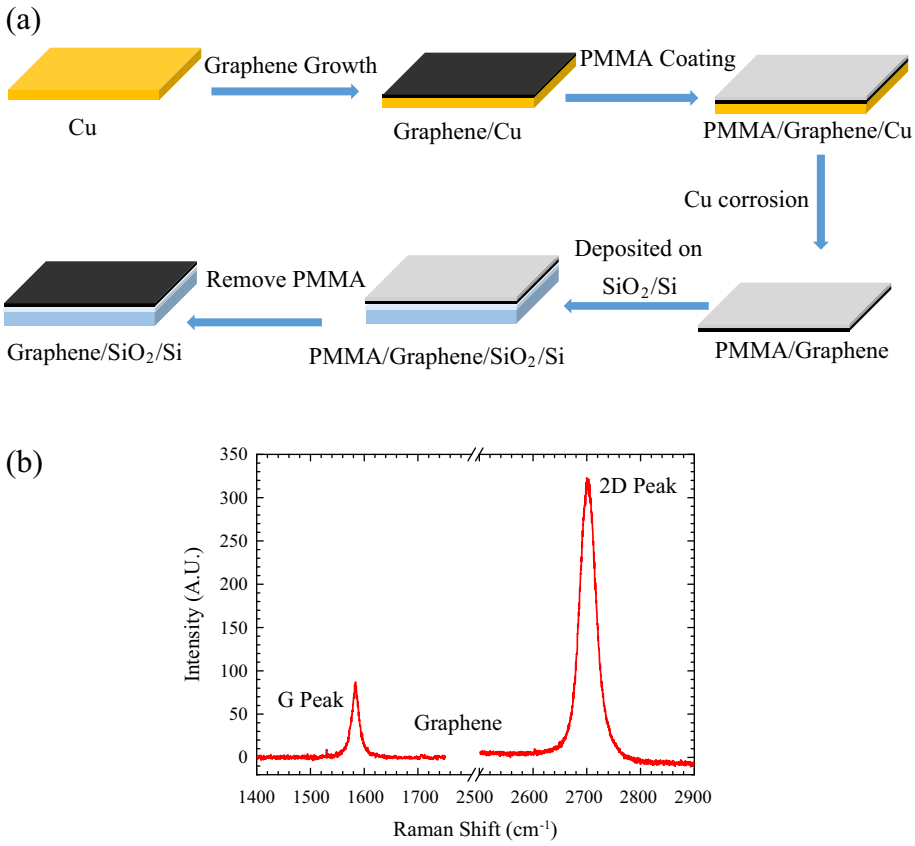

Fig. 2. (a) The process for the synthesis of monolayer graphene and sample preparation for the interface material: graphene was synthesized via conventional CVD method and was deposited on silicon wafer to get the interface structure. (b) Raman spectrum is used to characterize the quality of graphene sample. The intensity ratio of G peak to 2D peak can be used to define layer number. Raman characterization of graphene sample shows that the ratio is around 0.11, which indicates that the graphene synthesized in this measurement is monolayer structure.

experiments are needed in each measurement for the unique temperature coefficient of Raman peaks.

Raman shifts have inverted dependence on the temperatures for both graphene and silicon. The shifts of peaks are determined by fitting the peaks as shown in Fig. 3(a). The relationships between Raman shifts and temperatures of graphene layer and Si layer are calibrated in our measurement as shown in Fig. 3(b). The temperature coefficients against Raman shifts of peak for silicon and G peak for single-layer graphene are obtained as $t_{Si} = -0.026\ \mathrm{cm^{-1}/K}$ and $t_g = -0.031 \pm 0.005\ \mathrm{cm^{-1}/K}$ respectively as shown in Fig. 3(b). Tang et al. reported that the fitting slope for temperature against Raman shift for Si was $-0.022\ \mathrm{cm^{-1}/K}$ [35]. The temperature coefficient of single-layer graphene was revealed as $-0.025\ \mathrm{cm^{-1}/K}$ [34]. The calibration results for silicon and single-layer graphene in our work are comparable with the literatures in consideration of difference in experimental conditions and qualities of materials.

3.2. Result and discussion for thermal transport of graphene/SiO_2 interface

The temperatures of graphene layer and silicon layer can be determined from Raman peaks as shown in Fig. 1(b). It is noticed that the temperature of SiO_2 layer can't be obtained by Raman peaks due to its weak signal in the spectrum [20]. The interfacial thermal resistance between SiO_2 and Si is less than $8 \times 10^{-7}\ \mathrm{m^2K/W}$ [36], which can be calculated as $R_{Si/SiO_2} = A\Delta T_{Si/SiO_2}/Q$, where A is the contact area between Si layer and SiO_2 layer, $\Delta T_{Si/SiO_2}$ is the temperature drop between Si layer and SiO_2 layer, Q is the joule-heating power which approximates 1 W, respectively. Then the temperature drop between Si layer and SiO_2 layer is calculated as $\Delta T_{Si/SiO_2} = R_{Si/SiO_2} Q/A = 8 \times 10^{-3}$ K, which is so small that the temperature of Si layer can be regarded as the temperature of SiO_2 layer; in other words, the temperature of SiO_2 layer is obtained by the analysis of Raman spectrum of Si layer. Thus, the interfacial thermal conductance is calculated as $R_{g/SiO_2} = A\Delta T_{g/SiO_2}/Q$ with the measurements of steady temperature of graphene layer and Si layer by Raman thermometry under joule-heating. The temperature distribution of sample is displayed as Fig. 1(c). In order to reduce uncertainty in the measurements of interfacial thermal conductance, the linear relationships between joule-heating power and Raman shifts of Si and graphene are characterized as shown in Fig. 4(a). The slopes of Raman shifts against joule-heating power for Si and graphene are $q_{Si} = -0.691 \pm 0.063\ \mathrm{cm^{-1}/W}$ and $q_g = -1.824 \pm 0.186\ \mathrm{cm^{-1}/W}$ respectively. Thus, the interfacial thermal resistance can be calculated as $R_{g/SiO_2} = A \times d(T_g - T_{SiO_2})/dQ$ and derived as $A(q_g/t_g - q_{Si}/t_{Si})$ considering different power used in the experiment. Interfacial thermal resistance is characterized as $R_{g/SiO_2} = 2.94^{+1.9}_{-1.44} \times 10^{-3}$ m2 K/W, and the interfacial thermal conductance is obtained as $G_{g/SiO_2} = 340^{+327}_{-80}$ W/m K accordingly.

Table 1 lists selected works about interfacial thermal conductance measurements between graphene and substrates. The interfacial thermal conductance obtained in our experiment is small, which indicates that energy coupling between graphene and SiO_2 is poor. Quite lower interfacial thermal conductance can't be regarded as unreasonable result, since there have been very small values of interfacial thermal conductance in many interface sys-

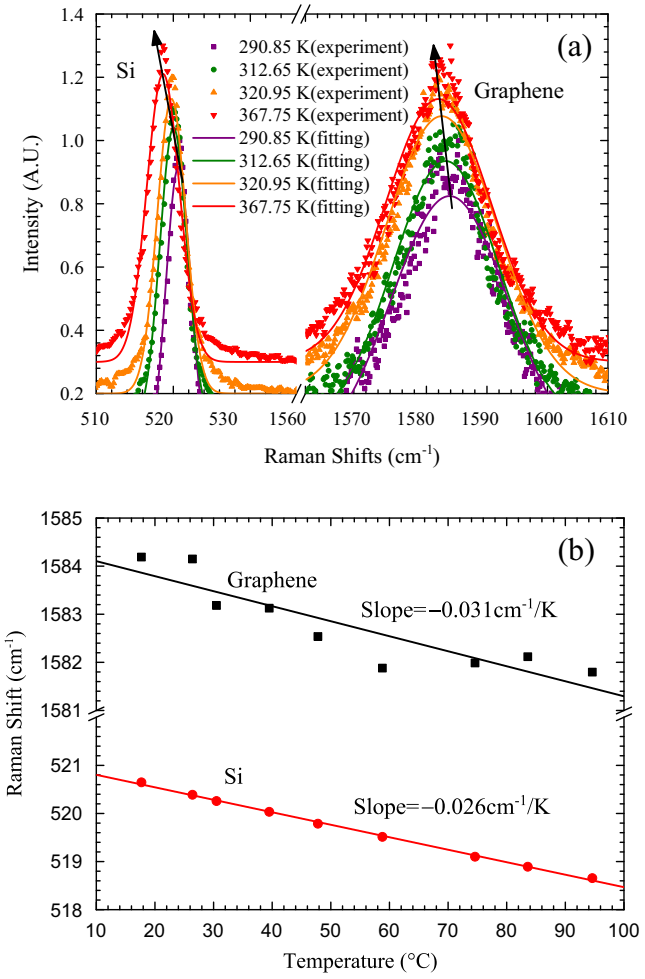

Fig. 3. (a) Raman peaks of silicon and G peaks of graphene are fitted by Gaussian function under different temperatures and there is obvious peaks shift with temperature. (b) The linear fittings between temperature and Raman shift of graphene and silicon. The slopes are displayed which indicate that Raman shifts have inverted dependence on temperature for both graphene and Si.

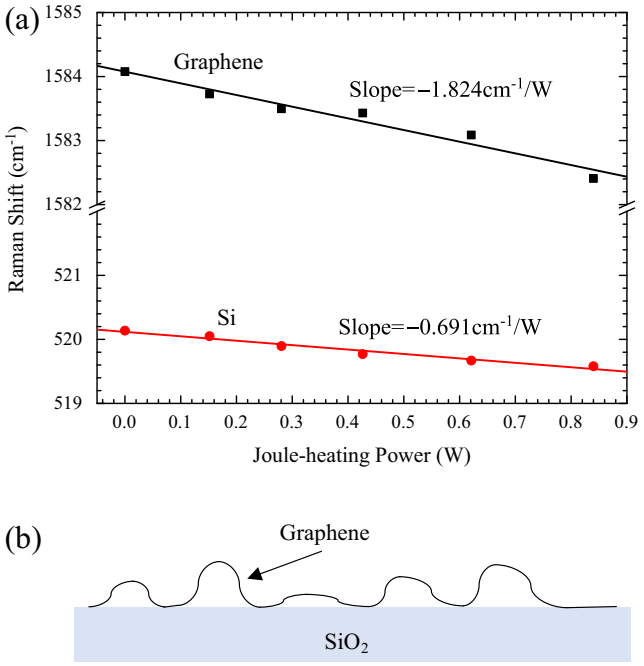

Fig. 4. (a) Measurement result and the linear fittings between Joule-heating power and Raman shift of graphene and silicon. The slopes are used for interface thermal conductance calculation. (b) The schematic for unconstrained contact between graphene layer and SiO_2 layer. The thermal stress in graphene layer and SiO_2 layer during Joule-heating exists and significant interface mismatch could happen due to different thermal expansion coefficients between graphene and SiO_2.

tems consisting of free ultrathin films which include graphene/Si [20] and graphene/boron nitride [37]. Thermal expansion coefficient of graphene is negative which is much different from that of SiO_2 [33]. Significant mismatch of thermal expansion coefficients between graphene and SiO_2 leads to thermal stress between graphene and SiO_2 during joule-heating. The thermal stress results in mechanical deformation of graphene, thus the situation of thermal transport across interface is much different due to the variation of morphology. The measured value of thermal conductance implies poor localized energy coupling at interface, therefore, it is reasonable to infer that the interface between graphene and SiO_2 has poor contact. In addition, the kinetic energy of graphene atoms is high at elevated temperatures, and many atoms would be beyond the range of van der Waals interaction from SiO_2 substrate, which might result in further deviation from SiO_2 substrate. Poor contact will be aggravated due to corrugation and wrinkling of graphene which are very common problem in CVD transfer graphene samples [38,39].

The situation of contact between graphene layer and SiO_2 substrate can be described as shown in Fig. 4(b) considering above mentioned factors such as thermal stress between graphene and SiO_2, larger energy of graphene atoms and corrugation problem in graphene, and unconstrained situation of graphene layer. It was reported that the thermal conductance decreases rapidly as the separation distance at interface increases [40]. As listed in Table 1, values of interfacial thermal conductance measured by Raman spectroscopy are smaller than that obtained by pump probe method and 3ω method. The coating of silicon dioxide layer on the top of graphene may contribute to high measured thermal conductance for the differential 3ω method. And there is metallic layer deposited on graphene for absorption of laser pulse and facilitating well-defined thermal probing in pump probe method. The metallic layer and oxide layer would influence the thermal transport across graphene/SiO_2 interfaces. The heat can transfer between the deposition layer and the substrate directly due to ultrathin thickness of monolayer graphene. The graphene/SiO_2 interfaces have minor effect on the thermal transport because there is atomic interaction between deposited layer atoms and substrate atoms [41]. In addition, the contact between graphene and substrate is well for constrained graphene deposited with layer in pump probe measurements and 3ω measurements. The contact between graphene and substrate is poor for unconstrained graphene in Raman spectroscopy measurements because the thermal stress between graphene and substrate might be significant during joule-heating; nevertheless, deposited layer on constrained graphene may improve the contact between graphene and substrate during coating layer. It is not strange that a large range of variation for the values of thermal conductance is shown in Table 1. Thus, the interfacial thermal conductance measured in our work is comparable with that in other works considering extremely loose contact and unconstrained graphene.

3.3. Result and discussion for in-plane thermal conductivity

Temperature gradient in the in-plane of graphene needs to be established in order to measure the thermal conductivity of graphene. Thus, the Raman probing laser is used to heat graphene and acts as a local heat source. Only a small portion of laser light

is absorbed by graphene. As shown in Fig. 5(a), the graphene layer absorbs a portion of laser power when the laser light passes through for the first time and most of the laser light penetrates through graphene layer and SiO_2 layer, then a portion of transmitted laser light is absorbed by silicon layer while the rest of them reflects back into graphene layer and the graphene layer absorbs another portion of laser light for the second time. In this calculation, the absorptivity of graphene for our wavelength used for calculation is 2.3% and the reflectance of graphene is less than 0.1% which is negligible [42]. The effect of SiO_2 layer on laser light can be totally ignored due to very small thickness of 300 nm and ultra-high light transmission coefficient of SiO_2 layer [29]. The ratio of laser light power absorbed by graphene at the first time is 2.3% and the rest 97.7% of laser power penetrates through graphene. 40% of transmitted light is reflected back into graphene layer and another 2.3% of reflected light is absorbed by the graphene layer for the second time. Thus, the total absorption ratio of laser light power by the graphene layer is 3.2%. The thermal conductivity of graphene is calculated from Eq. (1) by measuring the temperature rise at light spot of graphene. In order to reduce uncertainty in the measurement, the theoretical Eq. (1) is derived as

$$d\theta/dq = \frac{1}{2\pi k r_1 \delta m} \times \frac{K_0(mr_1)I_1(mr_2) + K_1(mr_2)I_0(mr_1)}{K_1(mr_1)I_1(mr_2) - K_1(mr_2)I_1(mr_1)} \quad (2)$$

The temperature distribution of three layers is illustrated in Fig. 5(b). The temperature rise of graphene under different laser-heating power is measured to calculate thermal conductivity. The linear relationship for Raman shift of graphene and Si against laser-heating power is fitted as shown in Fig. 6. Divided by the temperature coefficients of Raman shifts against temperatures for graphene $t_g = -0.031 \pm 0.005\ cm^{-1}/K$ and silicon $t_{Si} = -0.026\ cm^{-1}/K$, the linear fitting slopes of temperatures of graphene and silicon against laser power are $5.40^{+2.1}_{-1.5} \times 10^6$ K/W and $2.30^{+0.04}_{-0.04} \times 10^5$ K/W respectively, and the slope of temperature against laser power for silicon indicates the temperature of silicon almost remains unchanged with laser-heating. Since the thermal resistance of SiO_2 layer can be negligible, the temperature of SiO_2 layer is very close to that of Si layer. The effect of laser on heating SiO_2 layer is also negligible for non-laser absorption. With the geometry parameters, the measured interfacial thermal conductance and the local temperature rise under different laser-heating power, theoretical thermal conductivity curve of supported graphene is calculated as shown in Fig. 7. The thermal conductivity value of our sample is obtained as 179^{+111}_{-86} W/m K.

As listed in Table 2, thermal conductivity measurements of supported and suspended graphene have been reported. It has been validated that the thermal conductivity of supported graphene is

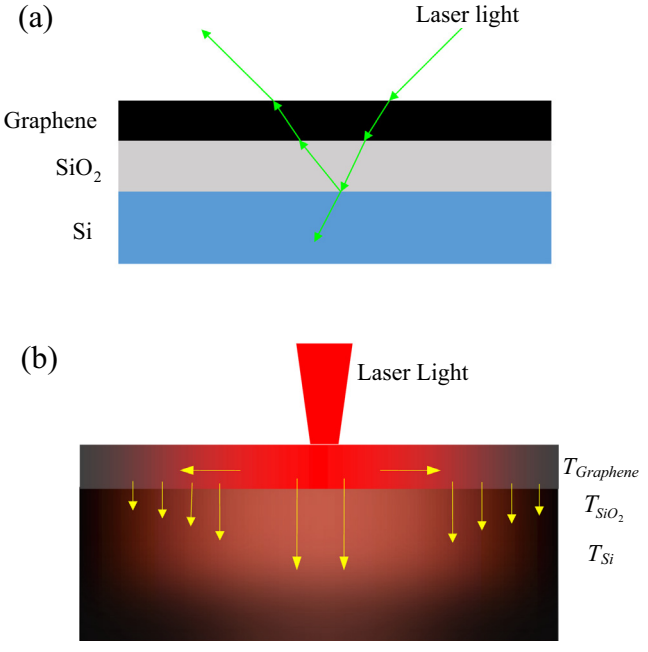

Fig. 5. (a) The illustration of laser transmission through different layers of graphene interface. (b) The diagrammatic drawing of temperature gradient under localized laser heating. The laser is focused on graphene layer and acts as a local heat source. The portion of heat dissipates along the graphene layer then down to substrate away from the heating point and other portion of heat dissipates directly through the interface down to substrate.

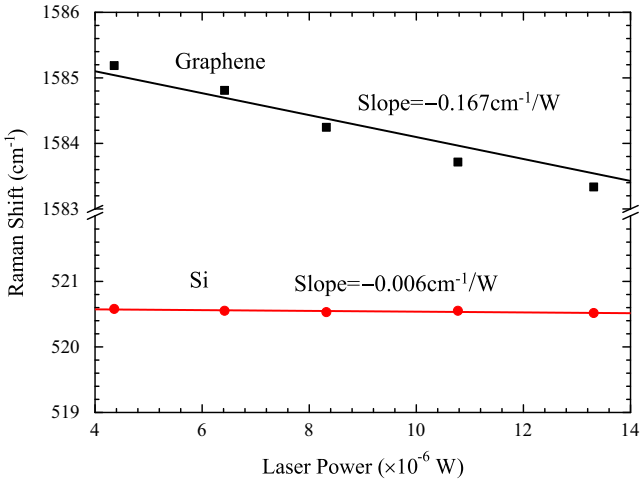

Fig. 6. The laser heating experimental result and the linear fitting between Raman shift of graphene and silicon and laser heating power. The slope of Raman shift against heating power for silicon indicates there is little temperature rise in silicon during laser heating. These slopes can be used to calculate the thermal conductivity of graphene.

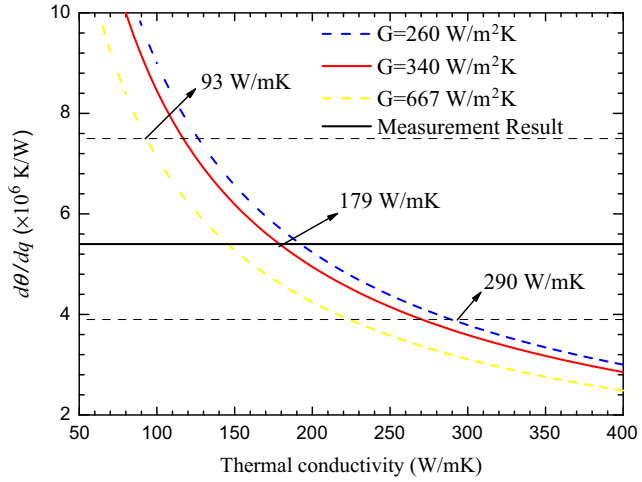

Fig. 7. The relationship between the ratio of temperature rise and absorbed laser power by graphene and theoretical thermal conductivity. The red solid line represents the relationship with measurement result for interfacial thermal conductance G, while the blue dashed line and yellow dashed line represent the relationship with the lower error limit and upper error limit for interfacial thermal conductance G respectively. The thermal conductivity is determined by the ratio of temperature rise and absorbed laser power by graphene and its error range. The dark solid line represents the measurement result of the ratio of temperature rise and absorbed laser power by graphene. (For interpretation of the references to colour in this figure legend, the reader is referred to the web version of this article.)

generally much smaller than that of suspended graphene. The existence of flexural ZA modes is contributed to the excellent thermal properties of graphene [4]. If graphene has contact with substrate, there are phonons leakage across the graphene/substrate interface and significant scattering of flexural ZA modes in supported graphene system, which suppress thermal conductivity of supported graphene greatly, while the flexural ZA modes contribute markedly to the thermal conductivity. In addition, the ripples in supported graphene are more obvious; in other words, the mechanical deformation of supported graphene is much severer than that of suspended graphene. The mechanical deformation of graphene would decrease thermal conductivity significantly. Thus, thermal conductivity of suspended graphene is much larger than that of supported graphene. Thermal conductivity reported by Balandin et al. [7] is much higher than that in other thermal conductivity measurements listed in Table 2. It was noticed that the absorptivity of single-layer graphene in the work by Balandin et al. was around 13%. Little difference in laser absorptivity would lead to much difference in thermal conductivity results.

It was reported that thermal transport in supported low-dimensional structure could be manipulated by modulating its coupling to the substrate [43,44]. The thermal conductivity of graphene would be enhanced by adjusting interaction between graphene and substrate. As mentioned above, the interfacial thermal conductance between graphene and SiO_2 in our work is measured as 340^{+327}_{-80} W/m^2 K, which means poor contact between graphene and SiO_2. Lower thermal conductivity in in-plane direction might be caused by serious phonons leakage and scattering. Another possible factor for the small value of thermal conductivity is that the sample in our work may be contaminated by the organic residues in the transfer process of PMMA membrane, and the thermal conductivity of graphene would be suppressed significantly with the organic residues [45]. Thus, much low thermal conductivity of supported graphene in our measurement is reasonable and comparable with other works considering above factors.

4. Conclusion

In this work, we developed an in-situ two-step approach based on Raman thermometry to investigate thermal transport in graphene/SiO_2 interface material. The two-step Raman approach incorporates a joule-heating experiment for interfacial thermal conductance characterization and a laser-heating experiment for thermal conductivity measurement. Results show that the thermal conductance of our unconstrained graphene/SiO_2 interface sample is 340^{+327}_{-80} W/m^2 K and thermal conductivity of this supported graphene is 179^{+111}_{-86} W/K. Terrible contact between graphene and SiO_2 substrate is responsible for the small value of interfacial thermal conductance. The phonons scattering and leakage at the graphene/SiO_2 interface is factor to suppress the thermal conductivity in graphene. This novel two-step Raman method makes it possible for localized characterization of both in-plane and out-of-plane thermal transport of 2D interface materials, which is important for comprehensively understanding the energy dissipation/phonon transport across such structures.

Acknowledgements

Y. Y. would like to thank the financial support from the National Natural Science Foundation of China (Nos. 51428603 and 51576145). S. W. acknowledges the support from the National Natural Science Foundation of China (No. 51375350).

References

[1] M. Forshaw, R. Stadler, D. Crawley, K. Nikoli, A short review of nanoelectronic architectures, Nanotechnology 15 (2004) S220–S223.
[2] B. Guo, L. Fang, B. Zhang, J.R. Gong, Graphene doping: a review, Insciences J. (2011) 80–89.
[3] M.M. Sadeghi, M.T. Pettes, L. Shi, Thermal transport in graphene, Solid State Commun. 152 (2012) 1321–1330.
[4] L. Lindsay, D.A. Broido, N. Mingo, Flexural phonons and thermal transport in graphene, Phys. Rev. B 82 (2010) 115427.
[5] L. Hu, T. Desai, P. Keblinski, Thermal transport in graphene-based nanocomposite, J. Appl. Phys. 110 (2011) 033517.
[6] B.D. Kong, S. Paul, M.B. Nardelli, K.W. Kim, First-principles analysis of lattice thermal conductivity in monolayer and bilayer graphene, Phys. Rev. B 80 (2009) 033406.
[7] A.A. Balandin, S. Ghosh, W. Bao, I. Calizo, D. Teweldebrhan, F. Miao, N.L. Chun, Superior thermal conductivity of single-layer graphene, Nano Lett. 8 (2008) 902–907.
[8] W.J. Evans, L. Hu, P. Keblinski, Thermal conductivity of graphene ribbons from equilibrium molecular dynamics: effect of ribbon width, edge roughness, and hydrogen termination, Appl. Phys. Lett. 96 (2010) 203112.
[9] F. Schwierz, Graphene transistors, Nat. Nanotechnol. 5 (2010) 487–496.
[10] M. Liang, B. Luo, L. Zhi, Application of graphene and graphene-based materials in clean energy-related devices, Int. J. Energy Res. 33 (2009) 1161–1170.
[11] G. Jo, M. Choe, S. Lee, W. Park, Y.H. Kahng, T. Lee, The application of graphene as electrodes in electrical and optical devices, Nanotechnology 23 (2012) 112001.
[12] E. Pop, V. Varshney, A.K. Roy, Thermal properties of graphene: fundamentals and applications, MRS Bull. 37 (2012) 1273–1281.
[13] J.H. Seol, I. Jo, A.L. Moore, L. Lindsay, Z.H. Aitken, M.T. Pettes, X. Li, Z. Yao, R. Huang, D. Broido, Two-dimensional phonon transport in supported graphene, Science 328 (2010) 213–216.
[14] W. Jang, Z. Chen, W. Bao, C.N. Lau, C. Dames, Thickness-dependent thermal conductivity of encased graphene and ultrathin graphite, Nano Lett. 10 (2010) 3909–3913.
[15] J. Chen, G. Zhang, B. Li, Substrate coupling suppresses size dependence of thermal conductivity in supported graphene, Nanoscale 5 (2013) 532–536.
[16] R. Mao, B.D. Kong, K.W. Kim, T. Jayasekera, A. Calzolari, M. Buongiorno Nardelli, Phonon engineering in nanostructures: controlling interfacial thermal resistance in multilayer-graphene/dielectric heterojunctions, Appl. Phys. Lett. 101 (2012) 113111.
[17] M. Li, J. Zhang, X. Hu, Y. Yue, Thermal transport across graphene/SiC interface: effects of atomic bond and crystallinity of substrate, Appl. Phys. A 119 (2015) 415–424.
[18] Z. Chen, W. Jang, W. Bao, C.N. Lau, C. Dames, Thermal contact resistance between graphene and silicon dioxide, Appl. Phys. Lett. 95 (2009) 161910.
[19] Y.K. Koh, M.H. Bae, D.G. Cahill, E. Pop, Heat conduction across monolayer and few-layer graphenes, Nano Lett. 10 (2010) 4363–4368.
[20] X. Tang, S. Xu, J. Zhang, X. Wang, Five orders of magnitude reduction in energy coupling across corrugated graphene/substrate interfaces, ACS Appl. Mater. Interfaces 6 (2014) 2809–2818.
[21] W. Cai, A.L. Moore, Y. Zhu, X. Li, S. Chen, L. Shi, R.S. Ruoff, Thermal transport in suspended and supported monolayer graphene grown by chemical vapor deposition, Nano Lett. 10 (2010) 1645–1651.
[22] J. Judek, A.P. Gertych, M. Swiniarski, A. Lapinska, A. Duzynska, M. Zdrojek, High accuracy determination of the thermal properties of supported 2D materials, Sci. Rep. 5 (2015) 12422.
[23] T.L. Bergman, F.P. Incropera, D.P. DeWitt, A.S. Lavine, Fundamentals of Heat and Mass Transfer, John Wiley & Sons, 2011.
[24] Y. Yue, X. Huang, X. Wang, Thermal transport in multiwall carbon nanotube buckypapers, Phys. Lett. A 374 (2010) 4144–4151.
[25] Y. Yue, G. Eres, X. Wang, L. Guo, Characterization of thermal transport in micro/nanoscale wires by steady-state electro-Raman-thermal technique, Appl. Phys. A 97 (2009) 19–23.
[26] X. Tang, Y. Yue, X. Chen, X. Wang, Sub-wavelength temperature probing in near-field laser heating by particles, Opt. Express 20 (2012) 14152–14167.
[27] Y. Yue, X. Wang, Nanoscale thermal probing, Nano Rev. 3 (2012) 11586.
[28] Y. Yue, X. Chen, X. Wang, Noncontact sub-10 nm temperature measurement in near-field laser heating, ACS Nano 5 (2011) 4466–4475.
[29] R. Kitamura, L. Pilon, M. Jonasz, Optical constants of silica glass from extreme ultraviolet to far infrared at near room temperature, Appl. Opt. 46 (2007) 8118–8133.
[30] D. Graf, F. Molitor, K. Ensslin, C. Stampfer, A. Jungen, C. Hierold, L. Wirtz, Spatially resolved Raman spectroscopy of single- and few-layer graphene, Nano Lett. 7 (2007) 238–242.
[31] X. Li, W. Cai, J. An, S. Kim, J. Nah, D. Yang, R. Piner, A. Velamakanni, Large-area synthesis of high-quality and uniform graphene films on copper foils, Science 324 (2016) 1312–1314.
[32] W. Liu, H. Li, C. Xu, Y. Khatami, K. Banerjee, Synthesis of high-quality monolayer and bilayer graphene on copper using chemical vapor deposition, Carbon 49 (2011) 4122–4130.
[33] D. Yoon, Y.W. Son, H. Cheong, Negative thermal expansion coefficient of graphene measured by Raman spectroscopy, Nano Lett. 11 (2011) 3227–3231.

[34] Y. Yue, J. Zhang, X. Wang, Micro/nanoscale spatial resolution temperature probing for the interfacial thermal characterization of epitaxial graphene on 4H-SiC, Small 7 (2011) 3324–3333.
[35] X. Tang, Y. Yue, X. Chen, X. Wang, Sub-wavelength temperature probing in nearfield laser heating by particles, Opt. Express 20 (2012) 14152–14167.
[36] O.W. Käding, H. Skurk, K.E. Goodson, Thermal conduction in metallized silicon-dioxide layers on silicon, Appl. Phys. Lett. 65 (1994) 1629.
[37] J. Zhang, Y. Hong, Y. Yue, Thermal transport across graphene and single layer hexagonal boron nitride, J. Appl. Phys. 117 (2015) 134307.
[38] T.M. Paronyan, E.M. Pigos, G. Chen, A.R. Harutyunyan, Formation of ripples in graphene as a result of interfacial instabilities, ACS Nano 5 (2011) 9619–9627.
[39] J.C. Meyer, A.K. Geim, M.I. Katsnelson, K.S. Novoselov, T.J. Booth, S. Roth, The structure of suspended graphene sheets, Nature 446 (2007) 60–63.
[40] H. Zhong, J.R. Lukes, Interfacial thermal resistance between carbon nanotubes: molecular dynamics simulations and analytical thermal modeling, Phys. Rev. B 74 (2006) 125403.
[41] Y. Yue, J. Zhang, X. Tang, S. Xu, X. Wang, Thermal transport across atomic-layer material interfaces, Nanotechnol. Rev. 4 (2015) 533–555.
[42] R.R. Nair, P. Blake, A.N. Grigorenko, K.S. Novoselov, T.J. Booth, T. Stauber, N.M. Peres, A.K. Geim, Fine structure constant defines visual transparency of graphene, Science 320 (2008) 1308.
[43] Z.X. Guo, D. Zhang, X.G. Gong, Manipulating thermal conductivity through substrate coupling, Phys. Rev. B 84 (2011) 075470.
[44] Z.Y. Ong, E. Pop, Effect of substrate modes on thermal transport in supported graphene, Phys. Rev. B 84 (2011) 075471.
[45] M.T. Pettes, I. Jo, Z. Yao, L. Shi, Influence of polymeric residue on the thermal conductivity of suspended bilayer graphene, Nano Lett. 11 (2011) 1195–1200.
[46] K.F. Mak, C.H. Lui, T.F. Heinz, Measurement of the thermal conductance of the graphene/SiO_2 interface, Appl. Phys. Lett. 97 (2010) 221904.
[47] P.E. Hopkins, M. Baraket, E.V. Barnat, T.E. Beechem, S.P. Kearney, J.C. Duda, J.T. Robinson, S.G. Walton, Manipulating thermal conductance at metal-graphene contacts via chemical functionalization, Nano Lett. 12 (2012) 590–595.
[48] H. Wang, K. Kurata, T. Fukunaga, H. Ago, H. Takamatsu, X. Zhang, T. Ikuta, K. Takahashi, T. Nishiyama, Y. Takata, Simultaneous measurement of electrical and thermal conductivities of suspended monolayer graphene, J. Appl. Phys. 119 (2016) 244306.
[49] J.U. Lee, D. Yoon, H. Kim, S.W. Lee, H. Cheong, Thermal conductivity of suspended pristine graphene measured by Raman spectroscopy, Phys. Rev. B 83 (2011) 081419.
[50] X. Xu, L.F. Pereira, Y. Wang, J. Wu, K. Zhang, X. Zhao, S. Bae, C. Tinh Bui, R. Xie, J. T. Thong, B.H. Hong, K.P. Loh, D. Donadio, B. Li, B. Ozyilmaz, Length-dependent thermal conductivity in suspended single-layer graphene, Nat. Commun. 5 (2014) 3689.
[51] C. Faugeras, B. Faugeras, M. Orlita, M. Potemski, R.R. Nair, A.K. Geim, Thermal conductivity of graphene in corbino membrane geometry, ACS Nano. 4 (2010) 1889–1892.
[52] Z. Wang, R. Xie, C.T. Bui, D. Liu, X. Ni, B. Li, J.T. Thong, Thermal transport in suspended and supported few-layer graphene, Nano Lett. 11 (2011) 113–118.